



**HAL**  
open science

## Structural characterization of IrisFP, an optical highlighter undergoing multiple photo-induced transformations

V. Adam, M. Lelimosin, S. Boehme, G. Desfonds, K. Nienhaus, M. Field, J. Wiedenmann, S. Mcsweeney, G. Nienhaus, D. Bourgeois

► **To cite this version:**

V. Adam, M. Lelimosin, S. Boehme, G. Desfonds, K. Nienhaus, et al.. Structural characterization of IrisFP, an optical highlighter undergoing multiple photo-induced transformations. Proceedings of the National Academy of Sciences of the United States of America, 2008, 105 (47), pp.18343-18348. 10.1073/pnas.0805949105 . hal-02389620

**HAL Id: hal-02389620**

**<https://hal.science/hal-02389620>**

Submitted on 7 Feb 2024

**HAL** is a multi-disciplinary open access archive for the deposit and dissemination of scientific research documents, whether they are published or not. The documents may come from teaching and research institutions in France or abroad, or from public or private research centers.

L'archive ouverte pluridisciplinaire **HAL**, est destinée au dépôt et à la diffusion de documents scientifiques de niveau recherche, publiés ou non, émanant des établissements d'enseignement et de recherche français ou étrangers, des laboratoires publics ou privés.



# Structural characterization of IrisFP, an optical highlighter undergoing multiple photo-induced transformations

Virgile Adam<sup>a</sup>, Mickaël Lelimosin<sup>b</sup>, Susan Boehme<sup>c</sup>, Guillaume Desfonds<sup>a</sup>, Karin Nienhaus<sup>c</sup>, Martin J. Field<sup>b</sup>, Joerg Wiedenmann<sup>d</sup>, Sean McSweeney<sup>a</sup>, G. Ulrich Nienhaus<sup>c,e,1</sup>, and Dominique Bourgeois<sup>a,b,1</sup>

<sup>a</sup>European Synchrotron Radiation Facility, 6 Rue Jules Horowitz, BP 220, 38043 Grenoble Cedex, France; <sup>b</sup>Institut de Biologie Structurale Jean-Pierre Ebel, Commissariat à l'Energie Atomique, Centre National de la Recherche Scientifique, Université Joseph Fourier, 41 Rue Jules Horowitz, 38027 Grenoble, France; <sup>c</sup>Institute of Biophysics, University of Ulm, Albert-Einstein-Allee 11, 89081 Ulm, Germany; <sup>d</sup>National Oceanography Centre, University of Southampton, Southampton SO14 3ZH, United Kingdom; and <sup>e</sup>Department of Physics, University of Illinois, Urbana, IL 61801

Edited by Hans Frauenfelder, Los Alamos National Laboratory, Los Alamos, New Mexico, and approved October 8, 2008 (received for review June 19, 2008)

**Photoactivatable fluorescent proteins (FPs) are powerful fluorescent highlighters in live cell imaging and offer perspectives for optical nanoscopy and the development of biophotonic devices. Two types of photoactivation are currently being distinguished, reversible photoswitching between fluorescent and nonfluorescent forms and irreversible photoconversion. Here, we have combined crystallography and (*in crystallo*) spectroscopy to characterize the Phe-173-Ser mutant of the tetrameric variant of EosFP, named IrisFP, which incorporates both types of phototransformations. In its green fluorescent state, IrisFP displays reversible photoswitching, which involves *cis-trans* isomerization of the chromophore. Like its parent protein EosFP, IrisFP also photoconverts irreversibly to a red-emitting state under violet light because of an extension of the conjugated  $\pi$ -electron system of the chromophore, accompanied by a cleavage of the polypeptide backbone. The red form of IrisFP exhibits a second reversible photoswitching process, which may also involve *cis-trans* isomerization of the chromophore. Therefore, IrisFP displays altogether 3 distinct photoactivation processes. The possibility to engineer and precisely control multiple phototransformations in photoactivatable FPs offers exciting perspectives for the extension of the fluorescent protein toolkit.**

fluorescent proteins | microspectrophotometry | photoactivation | photochromism | protein crystallography

In recent years, fluorescent proteins (FPs) from the green fluorescent protein (GFP) family have gained enormous popularity as genetically encoded fluorescence markers (1). They enable the visualization of a broad range of biological processes, including gene expression, protein translocation within cells, and cell movement during development. Photoactivatable FP variants have been recognized as particularly powerful imaging tools. Their fluorescence emission intensity or color can be controlled by irradiation with light of a specific wavelength, which allows selective highlighting of subsets of protein molecules within cells. This capability has been exploited in applications ranging from quantitative studies of protein movements in live cells (2, 3) to optical nanoscopy (4–6), and photoactivatable FPs may even be used in data-storage devices (7).

Two different groups of photoactivatable FPs are presently being distinguished. Members of the first group undergo reversible photoswitching between a fluorescent on state and a nonfluorescent off state (8–10), whereas members of the second group display irreversible photoconversion, either from a nonfluorescent to a fluorescent state (11–13) or between 2 fluorescent states with different emission wavelengths (14–19).

The structural basis of reversible photoswitching has been elucidated by crystallographic studies of several FPs including Dronpa (20), mTFP0.7 (9), and asFP595 (21). In the absence of light, the 4-(*p*-hydroxybenzylidene)-5-imidazolinone chro-

mophores of Dronpa and mTFP0.7 assume a *cis* conformation, in which the anionic, fluorescent state of the chromophore is predominant at physiological pH. Light-induced off-switching of the fluorescence was proposed to arise from a *cis-trans* photoisomerization of the chromophore accompanied by a change of its protonation state (22–24), a loss of chromophore planarity and, for mTFP0.7, a more disordered chromophore structure in the *trans* conformation (9). Alternatively, the loss of fluorescence in the off state was recently explained by light-induced protonation of the Dronpa chromophore, associated with increased chromophore flexibility, which enhances nonradiative deactivation pathways (25). In this scenario, *cis-trans* isomerization may occur as a side effect. In asFP595, the nonfluorescent *trans* state is thermodynamically more stable than the *cis* state, and light irradiation induces a *trans-cis* isomerization to the *cis* state (21), in which a minor, zwitterionic state has been proposed to promote fluorescence (26). When kept in the dark, reversibly photoswitching FPs relax within minutes to several hours to the thermodynamically more stable isomeric state.

For irreversible photoconversion, several mechanisms have been identified. For EosFP, a photoconverting FP that changes its emission color from green to red upon irradiation with violet light (18), the X-ray structures have been determined for the green and red forms (27, 28). They revealed a light-induced extension of the conjugated  $\pi$ -electron system of the chromophore, accompanied by a breakage of the protein backbone between the amide nitrogen and the  $\alpha$ -carbon of His-62 (EosFP residue numbering is used throughout this article), with surprisingly little change of the overall protein structure (27). Kaede (29), KikGR (17), and Dendra (14) are further representatives of green-to-red photoconverters that all share the tripeptide His-62–Tyr-63–Gly-64 as the chromophore-forming unit. A  $\beta$ -elimination reaction has been invoked to explain backbone cleavage, which may involve excited state proton transfer (ESPT) from the neutral chromophore to His-62 (27, 29), possibly assisted by dislocation of a water molecule (30). For PA-GFP (11) and PS-CFP (13), irreversible photoactivation

Author contributions: V.A., K.N., G.U.N., and D.B. designed research; V.A., M.L., S.B., and G.D. performed research; M.J.F., J.W., and S.M. contributed new reagents/analytic tools; V.A., M.L., S.B., and G.D. analyzed data; and V.A., M.L., K.N., G.U.N., and D.B. wrote the paper.

The authors declare no conflict of interest.

This article is a PNAS Direct Submission.

Data deposition: The atomic coordinates and structure factors have been deposited in the Protein Data Bank, www.pdb.org (PDB ID codes 2VVH, 2VVI, and 2VVJ).

<sup>1</sup>To whom correspondence may be addressed. E-mail: dominique.bourgeois@ibs.fr or uli@uiuc.edu.

This article contains supporting information online at [www.pnas.org/cgi/content/full/0805949105/DCSupplemental](http://www.pnas.org/cgi/content/full/0805949105/DCSupplemental).

© 2008 by The National Academy of Sciences of the USA

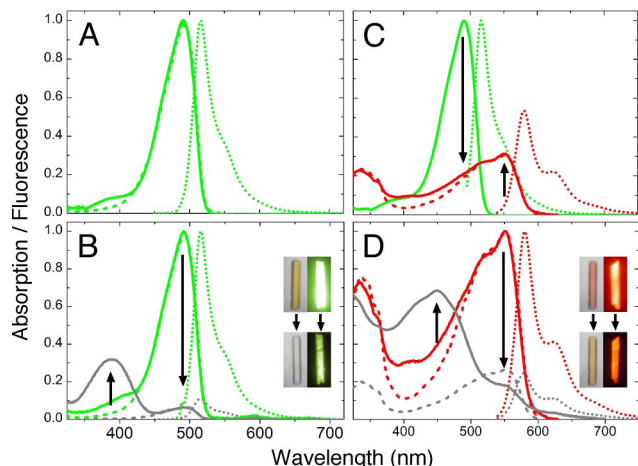


**Fig. 1.** Spectroscopic characterization of IrisFP. Absorption, excitation, and emission spectra scaled to equal maximum amplitudes are depicted by solid, dashed, and dotted lines, respectively. Emission spectra of green (red) IrisFP were obtained by exciting at 488 (532) nm. Excitation spectra of green (red) IrisFP were obtained by detecting at 550 (620) nm. (A) Green IrisFP. (B) Green IrisFP before (green lines) and after (gray lines) illumination with 488-nm light. (C) Red IrisFP (red lines) after photoconversion of green IrisFP (green lines) illumination with 405-nm light. (D) Red IrisFP before (red lines) and after (gray lines) illumination with 532-nm light. Spectra were recorded on solution samples in potassium phosphate buffer, pH 9. *Insets* show pictures of green IrisFP crystals before (B Upper) and after (B Lower) 488-nm illumination and of red IrisFP crystals before (D Upper) and after (D Lower) 532-nm illumination, respectively. Crystals are shown in bright-field mode (*Insets, Left*) and in fluorescence mode (*Insets, Right*). Detailed experimental procedures are provided in *SI Text*.

arises from stabilization of the anionic chromophore upon irradiation with violet light, presumably due to decarboxylation of Glu-212, as was earlier observed for GFP (31). Irreversible photoactivation has also been noticed for PA-mRFP1 (12) and the asFP595 Ala-148-Gly variant, also known as KFP1 (32); the underlying structural changes have yet to be elucidated.

The presence of structurally diverse photoactivation mechanisms suggests the intriguing possibility that multiple photo-transformations can be implemented within a single photoactivatable FP. Such a highlighter would enable sophisticated photoactivation schemes that could help unravel complex protein interaction patterns. Here, we introduce IrisFP, a variant of the tetrameric form of EosFP, which can be switched reversibly between fluorescent and nonfluorescent forms in its green state, then photoconverted from green to red, and finally switched reversibly between fluorescent and nonfluorescent forms in its

red state. A structural characterization of IrisFP based on a combination of X-ray crystallography and UV-visible spectrophotometry on crystal and solution samples provides a detailed picture of the different states of IrisFP at near-atomic level.

## Results

**Spectroscopic Characterization.** In the course of random mutagenesis experiments on EosFP, the mutant Phe-173-Ser was generated. We discovered that this mutant undergoes multiple photoactivation processes and, therefore, named it IrisFP (the Greek goddess Iris personifies the rainbow). Optical absorption and emission spectra of IrisFP solution samples and photographs of crystals recorded after exposure to a variety of illumination conditions are shown in Fig. 1. The corresponding spectra measured on single crystals are presented in [supporting information \(SI\) Fig. S1](#); spectroscopic parameters determined on solution samples are compiled in Table 1. In the green form of IrisFP (Fig. 1A and Fig. S1A), the main absorption band peaks at 487 nm; it is flanked by a vibronic shoulder at  $\approx 460$  nm. A minor absorption band resides at 390 nm. As for EosFP (18), the pH dependence of the absorption spectra (Fig. S2) reveals that the 487- and 390-nm bands are associated with the anionic and neutral states of the chromophore, respectively. Fluorescence emission, peaking at 516 nm, appears upon excitation of the anionic chromophore; the neutral form is only marginally fluorescent. The broader absorption/excitation bands of the anionic species [full width at half maximum (FWHM) 55 nm] as compared with EosFP (FWHM 25 nm) may reflect enhanced conformational freedom of the chromophore in IrisFP, which is also consistent with its decreased fluorescence quantum yield ( $\Phi = 0.43$ , Table 1).

Illumination of IrisFP solutions or crystals at room temperature by 488-nm light leads to pronounced changes in the optical spectra (Fig. 1B and Fig. S1B). The absorption band of the anionic species at 488 nm decays rapidly, concomitant with an increase of the band of the neutral species at 390 nm. A crisp isosbestic point at 426 nm (data not shown) suggests a light-driven conversion of the chromophore from anionic to neutral. The resulting species is essentially nonfluorescent. Such experiments are usually difficult to perform with crystals, owing to their high optical density (in IrisFP crystals, the penetration depth is only  $\approx 40 \mu\text{m}$  at 488 nm). Nevertheless, an almost complete loss of fluorescence can be achieved *in crystallo* because progressive deactivation of layers of molecules in the crystal ensures penetration of the actinic light into the bulk. The nonfluorescent state of the chromophore is very stable; it persists for hours in the dark ( $t_{1/2} \approx 5.5$  h in solution). The recovery (on switching) is markedly accelerated by illuminating with 405-nm light, occurring within seconds. The quantum yields for off and on switching are estimated as  $\Phi_{\text{off}} = 0.014$  and  $\Phi_{\text{on}} =$

**Table 1. Spectroscopic properties of IrisFP in solution**

Parameter	Green IrisFP	Red IrisFP	Green EosFP	Red EosFP
$\lambda_{\text{max, ex/em}}$ , nm	488 / 516	551 / 580	506 / 516	571 / 581
$\epsilon$ , $\text{M}^{-1} \text{cm}^{-1}$	52,200	35,400	72,000	41,000
QY <sub>fluorescence</sub>	$0.43 \pm 0.02$	$0.47 \pm 0.02$	$0.70 \pm 0.02$	$0.62 \pm 0.03$
QY <sub>off switching</sub> *	0.014	0.0020	—	—
QY <sub>on switching</sub> *	0.5	0.047	—	—
QY <sub>green-to-red conversion</sub>	0.0018	—	0.0008	—
Eff <sub>off</sub> †	$\approx 0.85$	$\approx 0.75$	—	—
$t_{1/2}$ , thermal recovery, h	5.5	3.2	—	—

Detailed experimental procedures are described in *SI Text*.  $\lambda_{\text{max}}$ , peak wavelength; ex, excitation; em, emission;  $\epsilon$ , extinction coefficient; QY, quantum yield;  $t_{1/2}$ , half-life.

\*Standard deviations are estimated as 25%.

†Switching efficiencies based on the following illumination conditions: Green IrisFP: 473 nm, 40 mW,  $\approx 10$  min. Red IrisFP: 532 nm, 50 mW,  $\approx 10$  min.

0.5, respectively. Off/on switching can be repeated several times in solution and in the crystal with minimal loss of fluorescence due to photobleaching (Fig. S3). Overall, the reversible switching behavior of green IrisFP resembles previous observations made with Dronpa (23) or mTFP0.7 (9), which suggests that IrisFP may undergo light-activated chromophore isomerization.

When stimulated by 405-nm laser light, the green IrisFP chromophore turns red (Fig. 1C and Fig. S1C). This photoconversion process gives rise to changes in the absorption and excitation spectra analogous to those reported earlier for the parent protein EosFP (18). The various bands can be assigned to differently charged chromophore species based on their response to pH changes (Fig. S2) and by comparison with EosFP. The excitation spectrum shows that the anionic species absorbs at 551 nm (with a vibronic shoulder at  $\approx 515$  nm) and fluoresces at 580 nm, whereas the neutral species, with a broad absorption feature at  $\approx 450$  nm, does not contribute to the fluorescence at 580 nm. Higher-order electronic transitions of the red chromophore are visible in the spectral region  $<400$  nm. Prolonged exposure to violet light results in a slow decay of red fluorescence, possibly due to photobleaching. However, as a result of intramolecular Förster resonance energy transfer (FRET) from green to red subunits within the tetramer, already a moderate 405-nm light exposure yields an almost complete change to red fluorescence. The quantum yield of photoconversion is enhanced as compared with that of the parent protein ( $\Phi_{\text{green/red}} = 1.8 \times 10^{-3}$ , Table 1).

Exposure of red-converted IrisFP to green light (532 nm) induces yet another photoswitching event, characterized by a decrease in the red fluorescence (Fig. 1D and Fig. S1D). Concomitantly, absorption at 551 nm decreases and absorption at 450 nm increases, which suggests that a neutral form of the chromophore becomes stabilized. Under our experimental conditions, a maximum switching yield of  $\approx 75\%$  could be achieved (Table 1). In the dark, the new species slowly reverts to the red fluorescent state ( $t_{1/2} \approx 3.2$  h). The return is strongly accelerated by exposure to 440-nm light. As for the green species, off/on switching can be repeated several times in solution and in the crystal with minimal loss of fluorescence due to photobleaching (Fig. S3). The quantum yields of photoactivated off and on switching of the red form are estimated to be  $\Phi_{\text{off}} = 0.0020$  and  $\Phi_{\text{on}} = 0.047$ , respectively. Interestingly, at moderate levels of photoconversion to the red form, off-switching of the red fluorescence results in an increase in green fluorescence (Fig. S4), which arises from the loss of intramolecular energy transfer from green to red monomers within tetrameric molecules.

**X-Ray Crystallographic Characterization.** To reveal the structural basis of the spectroscopically observed photoactivation processes in IrisFP, we performed X-ray structure analyses on crystals that were exposed to light conditions chosen to enhance particular species. Data collection and refinement statistics are compiled in Table S1. The X-ray structure of the green form of IrisFP, crystallized in the dark, was determined at a resolution of 1.8 Å without prior light exposure. The asymmetric unit consists of a well-defined tetramer. The individual subunits of IrisFP show the classical  $\beta$ -can fold, with no major deviation from the EosFP structure (27), as indicated by the backbone rms deviation of 0.36 Å between the 2 models. The anionic chromophore is slightly nonplanar (Table S1), which may account for the lower fluorescence quantum yield as compared with EosFP (Table 1). The phenolate moiety is stabilized by a hydrogen bond to Ser-142 and 2 water molecules (W-2188 and W-2017, Fig. 2 and S5A). The remarkable photoactivation properties of IrisFP result from the replacement of Phe-173 by serine. In EosFP, Phe-173 forces the side chain of Met-159 to establish van der Waals contact with the hydroxybenzylidene moiety (Fig. 2). The smaller Ser-173 side chain in IrisFP reduces these steric con-

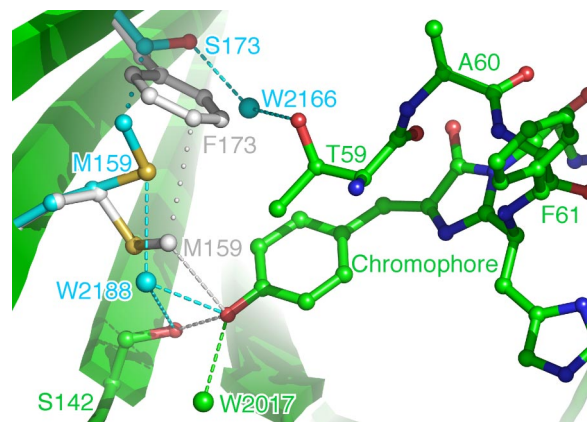


**Fig. 2.** Changes in the chromophore environment induced by the F173S mutation in EosFP. Common structural elements of EosFP and IrisFP are represented with green carbon atoms. Residues Phe-173 and Met-159 in EosFP are represented with gray carbon atoms, whereas the mutated residue Ser-173 and residue Met-159 in IrisFP are represented with cyan carbon atoms. The 2 water molecules (W-2188 and W-2166) are represented with cyan spheres, and W-2017 is represented with a green sphere. Hydrogen bonds are shown with dashed lines and van der Waals interactions with dotted lines.

straints, and the Met-159 side chain rotates away from the chromophore. Two cavities are created (total volume  $\approx 13$  Å<sup>3</sup>), each filled with a water molecule (W-2188 and W-2166, Fig. 2). The less-densely packed chromophore environment of IrisFP may lead to enhanced flexibility of the chromophore, which is in line with the spectroscopic observations that, compared with EosFP, the absorption and emission bands are broader and the fluorescence quantum yield is reduced.

To examine the structural basis of photoswitching of the green form of IrisFP, we illuminated a green crystal with 488-nm laser light and flash-cooled it immediately afterward. A diffraction dataset was collected to a resolution of 2.0 Å. An electron density omit map is shown in Fig. S5B. From the superposition of the refined models of the fluorescent and nonfluorescent forms in Fig. 3A, it is evident that off switching is accompanied by a *cis-trans* isomerization of the chromophore, as was earlier reported for Dronpa (20) and mTFP0.7 (9). The *trans* isomer of the chromophore is nonplanar (Table S1). Substantial rearrangements of residues Ser-142, His-194, Glu-212, Arg-66, and Ile-157 in the chromophore cavity are also apparent (Fig. 3A). The hydrogen bond between the phenolate oxygen of the *cis* chromophore and the Ser-142 hydroxyl side chain is removed and Ser-142 achieves a double conformation, either reorienting toward the solvent or H-bonding to His-194 and W-2188. The *trans* chromophore hydrogen-bonds to the presumably deprotonated carboxylate group of Glu-144 and to W-2032, most probably assuming a protonated phenolic form consistent with the observed loss of fluorescence and the increased absorption at 390 nm. The hydrogen-bonding network linking Glu-212 and Glu-144 via His-194 in the *cis* conformation involves Arg-66 in the *trans* conformation, implying large conformational rearrangements of the latter 2 residues similar to those observed in Dronpa (20) or mTFP0.7 (9). In addition, the side chain of Ile-157 undergoes a flip of  $\approx 145^\circ$ , possibly because of transient repulsion during chromophore isomerization. Based on these structures, the enthalpy difference between the 2 isomeric forms of green IrisFP was estimated from QM/MM molecular dynamics as 68 kJ/mol (SI Text and Table S2). This value is substantially smaller than the one estimated for EosFP (114 kJ/mol), assuming a similar *trans* structure. Calculations performed with null atomic charges for Ser-142 suggest that the stability of the *trans* isomeric state largely depends on the electrostatic interactions

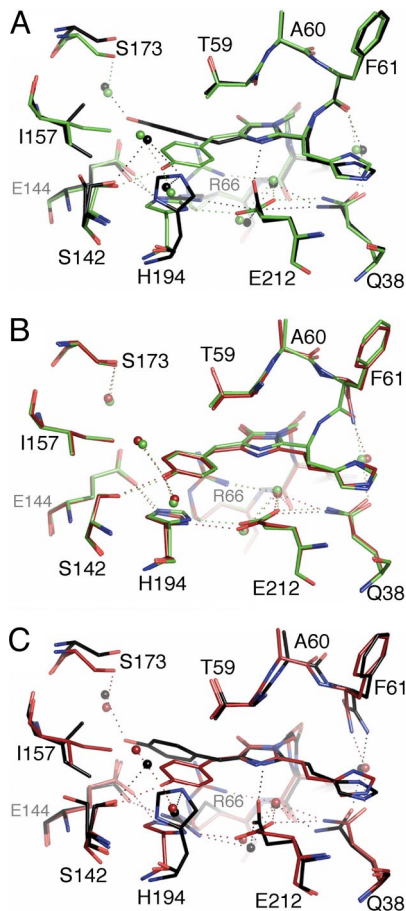


**Fig. 3.** Structural changes of the chromophore pocket upon phototransformation of IrisFP. (A) Superposition of the native green state (green) and the first reversibly switched state (black) obtained upon illumination at 488 nm. (B) Superposition of the native green state (green) and the irreversibly photoconverted red state (red) obtained after illumination at 405 nm. (C) Superposition of the red state (red) with the second reversibly switched state (black) obtained upon illumination at 405 nm, followed by illumination at 532 nm. In C, a putative model of the *trans* state of red IrisFP is shown (black). Hydrogen bonds are shown as dotted lines. Water molecules are shown as spheres.

between this residue and its environment. These interactions are much more favorable in IrisFP than in EosFP (Table S3). Diffraction data collected on a green IrisFP crystal after recovery in the dark from the off state confirmed the reversibility of the *cis*–*trans* isomerization, as the resulting structure was indistinguishable from the one of the initial fluorescent state (data not shown).

To determine the structure of red IrisFP, a green crystal was illuminated by 405-nm light and flash-cooled to collect a diffraction dataset at 2.0-Å resolution. Backbone cleavage between Phe-61 and His-62 was firmly established on the basis of omit electron density maps (Fig. S5C). Except for this modification, the superposition of the modeled chromophore environments of the green and red forms in Fig. 3B shows a nearly unperturbed chromophore pocket, as was observed earlier for red EosFP (27). A water molecule proximal to His-62 is dislocated in the red form, as was recently also reported for Kaede (30). These results support the notion of identical green-to-red photoconversion mechanisms for IrisFP and EosFP. Signs of radiation damage that could be caused by the long violet-light exposure of the sample, such as decarboxylation of Glu-212, were not noticeable.

To investigate the structural basis of reversible photoswitching of the red form of IrisFP, a green crystal was irreversibly

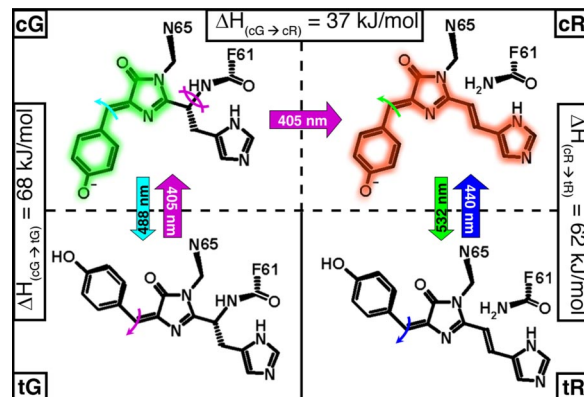


**Fig. 4.** Photoinduced transformations in IrisFP. Structural motions induced by light are represented by curved arrows of the same color as those used to represent light illumination at specific wavelengths. CG, *cis*-green Iris; tG, *trans*-green Iris; cR, *cis*-red Iris; tR, *trans*-red Iris.

photoconverted to the red form by illumination with 405-nm light and subsequently exposed to 532-nm light to induce reversible switching. After flash-cooling, diffraction data were collected to 2.2-Å resolution. In addition to the features characteristic of green-to-red photoconversion of IrisFP, the electron density map shows the *p*-hydroxybenzylidene ring in both the *cis* and *trans* conformations (Fig. S5D). This observation suggests a partial *cis*–*trans* isomerization of the chromophore, with features similar to those displayed by green off-switched IrisFP (Fig. 3A). However, the multiple conformations coexisting in the crystal, possibly as a result of limited penetration of green light within the crystal, made a reliable structural refinement difficult. Thus, assuming a *trans* conformation of the chromophore, only a tentative, energy-minimized model of the off-switched state could be produced (Fig. 3C and Fig. S5D). Based on this model, the enthalpy difference between the 2 isomeric states of red IrisFP was calculated to be 62 kJ/mol (Table S2). As for the green form, this difference is much higher for wild-type EosFP (122 kJ/mol) because of the less-favorable interactions of Ser-142 with its environment.

## Discussion

From the spectroscopic and crystallographic data presented here, it is evident that 2 photoactivation mechanisms occur in IrisFP: reversible photoswitching between a fluorescent and a nonfluorescent state, based on *cis*–*trans* isomerization of the chromophore, and irreversible green-to-red photoconversion between 2 different fluorescent forms of the chromophore. Fig. 4 summarizes the different optical states of IrisFP, highlighting the richness of its photophysics.

Superposition of the structures of IrisFP, Dronpa, and mTFP0.7 in their fluorescent *cis* and nonfluorescent *trans* states (Fig. S6) suggests that reversible photoisomerization in these proteins proceeds by similar mechanisms. In all 3 proteins, rotation of the chromophore is coupled to concerted motions of His-194 and Arg-66. Glu-212 and Glu-144 act as nanotweezers, providing hydrogen bonds to His-194 in the *cis* configuration and to Arg-66 in the *trans* configuration and, thereby, stabilizing both conformations. However, this common configuration is clearly not sufficient to enable photoswitching, as it is also found in the *cis* state of nonphotoswitchable FPs such as EosFP or Kaede (29). Stabilization of the *trans* conformation of the chromophore requires additional interactions that, in particular, compensate for the cost of breaking the hydrogen bond linking the phenolate oxygen of the benzylidene group to Ser-142 in the *cis* state. Comparison between EosFP and IrisFP allows a precise identification of these additional interactions. Our enthalpy calcu-

lations (Table S3) suggest that an essential factor is the availability of a polar environment around Ser-142 in the *trans* state. In IrisFP, such an environment is provided by the repositioning of Met-159 and by the introduction of water molecule W-2188. As a consequence, Ser-142 may either hydrogen-bond to His-194 and W-2188 or reorient toward the solvent. Our molecular-dynamics simulations suggest that these 2 options are prohibited in EosFP because of the hydrophobic character of Met-159 residing in close vicinity of Ser-142 (Table S2 and Table S3). In Dronpa and mTFP0.7, Ser-142 is also observed to find hydrogen-bonding partners inside the barrel or to reorient toward the solvent in the *trans* configuration of the chromophore. Thus, there are several structural solutions to the problem of stabilizing Ser-142 (Fig. S6): in comparison with EosFP, Dronpa has a valine instead of Ile-157, mTFP0.7 a histidine instead of Met-159, and IrisFP a serine instead of Phe-173.

Another factor contributing to the stability of the *trans* state is the network of interactions available around the phenolic oxygen of the chromophore's benzylidene moiety in this state. In IrisFP, the phenolic oxygen is stabilized by Glu-144 and water molecule W-2032, which both provide hydrogen bonding. Therefore, in contrast to Dronpa and mTFP0.7, the chromophore environment in the *trans* conformation appears largely polar.

Whereas bistability is an essential property of photoswitchable FPs, efficient photoswitching requires a low transition barrier between the 2 isomeric states. Free space around the *p*-hydroxybenzylidene moiety of the chromophore can clearly influence the photoswitching kinetics. The superposition of the *cis* forms of EosFP, Dronpa, and mTFP0.7 (Fig. S6A) reveals that these proteins provide rather similar steric environments around the chromophore. In contrast, in IrisFP, the mutation Phe-173-Ser creates significantly more space around the chromophore, notably by displacing Met-159 (Fig. 2). This observation might relate to the exceptional switching quantum yields measured for this protein. Interestingly, the Dronpa mutant Met-159-Thr shows substantially faster photoswitching kinetics than Dronpa (33). Presumably, even more space is freed around the chromophore in this variant, further lowering the transition barrier at the expense of a much reduced fluorescence quantum yield.

It is interesting to note that the 3 proteins compared in Fig. S6 have a different first amino acid in the chromophore-forming triad, namely cysteine in Dronpa, histidine in IrisFP, and alanine in mTFP0.7. Therefore, on/off switching by photoisomerization apparently does not depend on the nature of this amino acid. We also noticed that the carboxylate group of Glu-212 in IrisFP rotates by 90° upon isomerization and forms a hydrogen bond to the presumably unprotonated nitrogen of the chromophore's imidazolinone moiety, contrary to what is observed in Dronpa or mTFP0.7. Therefore, Glu-212 in the neutral *trans* chromophore configuration appears to be protonated. Assuming that this residue is also protonated in the neutral *cis* chromophore configuration, this observation may implicate Glu-212 as a potential donor of a proton in the putative  $\beta$ -elimination reaction leading to green-to-red photoconversion in EosFP-type proteins (27, 29). In the *trans* configuration of green IrisFP, the Glu-212 carboxylate side chain appears too far removed from His-62 for efficient proton transfer (Fig. 3A). Therefore, green-to-red photoconversion is unlikely to occur from the neutral *trans* state. Rather, absorption of a violet photon may lead to deprotonation of the phenol oxygen (via excited-state proton transfer), favoring back-isomerization to the *cis* state, from which photoconversion to the red form may readily occur. The excited-state behavior of photoactivatable proteins is to a large extent determined by the protonation states of the chromophore and its environment (23, 26). Therefore, more detailed investigations of these protonation states and their interplay with

isomerization will be required to decipher the photoactivation mechanisms of IrisFP.

One could be concerned that the presence of multiple phototransformations in IrisFP would result in poor yields for each of them and in a high susceptibility to photobleaching. However, reversible photoswitching in green IrisFP displays a remarkable efficiency compared with other Dronpa-like proteins. The yield of green-to-red photoconversion is also slightly increased compared with its parent protein EosFP, although red IrisFP appears more susceptible to photobleaching than EosFP. However, upon illumination with violet light, no chromophore photodamage is apparent in our crystal structures.

Our structural data suggest that the mechanisms for reversible photoswitching are essentially the same for green and red IrisFP, although the inhomogeneous chromophore conformation in the X-ray structure of photoswitched red IrisFP still leaves some possibility that isomerization may not be strictly required for switching in this state, as suggested for Dronpa (25). From the backbone breakage next to the chromophore in red IrisFP, which has also been noticed for the photoisomerizable marker protein asFP595 (21), one may expect an enhanced conformational flexibility of the chromophore and thus a facilitated light-induced isomerization. We noticed, on the contrary, that red IrisFP can be photoswitched to the nonfluorescent *trans* form slightly less efficiently than green IrisFP.

Incomplete green-to-red photoconversion may pose some limitations in one or the other marker application. Nevertheless, these adverse effects are greatly alleviated in the tetrameric form of IrisFP if we deliberately choose to only partially photoconvert the marker proteins in the sample. The strong FRET coupling between the chromophores in the tetramer leads to red fluorescence emission upon excitation of the green chromophores even if only 1 of the 4 chromophores is converted into its red fluorescent *cis* form (34). Off switching of the red form then results in the reappearance of green emission because the *trans* configuration of the neutral red chromophore does not absorb green light (Fig. S4). Thus, the partially red-converted tetramer effectively shows an interconversion between 2 bright states, red and green (Fig. S7). Such a mechanism is reminiscent of a technique used in DsRed to induce a color change (35) and also relates to the recently designed protein Phamret (36). It could be exploited further in tandem dimer constructs.

To turn IrisFP into a widely applicable highlighter protein, we aim to develop a monomeric version by introducing similar modifications as in EosFP (18), hoping that it will exhibit the same multiple photoactivation processes that we have observed here for the tetramer.

## Conclusions

Photoactivatable FPs hold great promises for applications in cell biology. However, reversibly photoswitchable FPs are not visible in their off state, and photoconvertible FPs are limited by the nonreversible nature of photoconversion. These drawbacks may be alleviated with new highlighters such as IrisFP, which combine the 2 modes of photoactivation. Other applications taking advantage of the multiple phototransformations displayed by IrisFP will undoubtedly emerge, including two-color nanoscopy and sequential photoactivation schemes that can be beneficial for unraveling complex protein–protein interactions. IrisFP also hints at the possibility to combine read-only and rewritable capabilities in future mass storage media.

## Materials and Methods

The experimental procedures are briefly sketched in the following; a detailed description is provided as *SI Text*. IrisFP was overexpressed and purified as EosFP (18). Rod-shaped crystals ( $0.2 \times 0.2 \times 0.8$  mm<sup>3</sup>) were grown at 20 °C in 2.4 M ammonium sulfate, 0.1 M bicine (pH 8.4).

X-ray data were collected at 100 K at the European Synchrotron Radiation Facility (ESRF). Crystal structures of IrisFP were solved by molecular replacement using EosFP as a starting model. To induce phototransformations, crystals were illuminated in their crystallization drops before flash-cooling. Illumination conditions are described in *SI Text*.

Spectra on solutions were taken at room temperature, by using protein concentrations of  $\approx 10 \mu\text{M}$  (absorption) and  $1 \mu\text{M}$  (fluorescence) in 100 mM potassium phosphate buffer (pH 9.0). *In crystallo* spectroscopy was carried out at 100 K by using the microspectrophotometer of the Cryobench laboratory (37).

Enthalpy differences between pairs of phototransformed states in IrisFP and wild-type EosFP were calculated with the *fDynamo* library (38), by using a QM/MM potential. The chromophore and the His-194 and Glu-212 side

chains were in the QM region, and the remaining atoms were in the MM region. Enthalpy differences were estimated in 2 ways, by energy minimization of single structures and by Langevin molecular dynamics at 300 K for 100 ps with a time step of 1 fs.

**ACKNOWLEDGMENTS.** The European Synchrotron Radiation Facility is acknowledged for support of the Cryobench laboratory and for providing in-house beam time on beamlines ID14-3, ID23-1, and ID29. This work was supported by Agence Nationale de la Recherche Grant ANR-07-BLAN-0107-01 (to D.B.), Deutsche Forschungsgemeinschaft Grants NI 291/9 and SFB 497 (to G.U.N.), the Fonds der Chemischen Industrie (G.U.N.), and the Landesstiftung Baden-Württemberg (Elite Postdoc Program) (J.W.).

1. Shaner NC, Patterson GH, Davidson MW (2007) Advances in fluorescent protein technology. *J Cell Sci* 120:4247–4260.
2. Lukyanov KA, Chudakov DM, Lukyanov S, Verkhusha VV (2005) Innovation: Photoactivatable fluorescent proteins. *Nat Rev Mol Cell Biol* 6:885–891.
3. Wiedenmann J, Nienhaus GU (2006) Live-cell imaging with EosFP and other photoactivatable marker proteins of the GFP family. *Exp Rev Proteomics* 3:361–374.
4. Hess ST, Girirajan TP, Mason MD (2006) Ultra-high resolution imaging by fluorescence photoactivation localization microscopy. *Biophys J* 91:4258–4272.
5. Betzig E, et al. (2006) Imaging intracellular fluorescent proteins at nanometer resolution. *Science* 313:1642–1645.
6. Hofmann M, Eggeling C, Jakobs S, Hell SW (2005) Breaking the diffraction barrier in fluorescence microscopy at low light intensities by using reversibly photoswitchable proteins. *Proc Natl Acad Sci USA* 102:17565–17569.
7. Sauer M (2005) Reversible molecular photoswitches: A key technology for nanoscience and fluorescence imaging. *Proc Natl Acad Sci USA* 102:9433–9434.
8. Ando R, Mizuno H, Miyawaki A (2004) Regulated fast nucleocytoplasmic shuttling observed by reversible protein highlighting. *Science* 306:1370–1373.
9. Henderson JN, Ai HW, Campbell RE, Remington SJ (2007) Structural basis for reversible photobleaching of a green fluorescent protein homologue. *Proc Natl Acad Sci USA* 104:6672–6677.
10. Lukyanov KA, et al. (2000) Natural animal coloration can be determined by a nonfluorescent green fluorescent protein homolog. *J Biol Chem* 275:25879–25882.
11. Patterson GH, Lippincott-Schwartz J (2002) A photoactivatable GFP for selective photolabeling of proteins and cells. *Science* 297:1873–1877.
12. Verkhusha VV, Sorkin A (2005) Conversion of the monomeric red fluorescent protein into a photoactivatable probe. *Chem Biol* 12:279–285.
13. Chudakov DM, et al. (2004) Photoswitchable cyan fluorescent protein for protein tracking. *Nat Biotechnol* 22:1435–1439.
14. Gurskaya NG, et al. (2006) Engineering of a monomeric green-to-red photoactivatable fluorescent protein induced by blue light. *Nat Biotechnol* 24:461–465.
15. Mizuno H, et al. (2003) Photo-induced peptide cleavage in the green-to-red conversion of a fluorescent protein. *Mol Cell* 12:1051–1058.
16. Oswald F, et al. (2007) Contributions of host and symbiont pigments to the coloration of reef corals. *FEBS J* 274:1102–1109.
17. Tsutsui H, Karasawa S, Shimizu H, Nukina N, Miyawaki A (2005) Semi-rational engineering of a coral fluorescent protein into an efficient highlighter. *EMBO Rep* 6:233–238.
18. Wiedenmann J, et al. (2004) EosFP, a fluorescent marker protein with UV-inducible green-to-red fluorescence conversion. *Proc Natl Acad Sci USA* 101:15905–15910.
19. Ivanchenko S, et al. (2007) Two-photon excitation and photoconversion of EosFP in dual-color 4Pi confocal microscopy. *Biophys J* 92:4451–4457.
20. Andresen M, et al. (2007) Structural basis for reversible photoswitching in Dronpa. *Proc Natl Acad Sci USA* 104:13005–13009.
21. Andresen M, et al. (2005) Structure and mechanism of the reversible photoswitch of a fluorescent protein. *Proc Natl Acad Sci USA* 102:13070–13074.
22. Habuchi S, et al. (2005) Reversible single-molecule photoswitching in the GFP-like fluorescent protein Dronpa. *Proc Natl Acad Sci USA* 102:9511–9516.
23. Habuchi S, et al. (2006) Photo-induced protonation/deprotonation in the GFP-like fluorescent protein Dronpa: Mechanism responsible for the reversible photoswitching. *Photochem Photobiol Sci* 5:567–576.
24. Fron E, et al. (2007) Ultrafast excited-state dynamics of the photoswitchable protein Dronpa. *J Am Chem Soc* 129:4870–4871.
25. Mizuno H, et al. (2008) Light-dependent regulation of structural flexibility in a photochromic fluorescent protein. *Proc Natl Acad Sci USA* 105:9227–9232.
26. Schäfer LV, Groenhof G, Boggio-Pasqua M, Robb MA, Grubmüller H (2008) Chromophore protonation state controls photoswitching of the fluoroprotein asFP595. *PLoS Comput Biol* 4:e1000034.
27. Nienhaus K, Nienhaus GU, Wiedenmann J, Nar H (2005) Structural basis for photo-induced protein cleavage and green-to-red conversion of fluorescent protein EosFP. *Proc Natl Acad Sci USA* 102:9156–9159.
28. Nienhaus GU, et al. (2006) Photoconvertible fluorescent protein EosFP: biophysical properties and cell biology applications. *Photochem Photobiol* 82:351–358.
29. Ando R, Hama H, Yamamoto-Hino M, Mizuno H, Miyawaki A (2002) An optical marker based on the UV-induced green-to-red photoconversion of a fluorescent protein. *Proc Natl Acad Sci USA* 99:12651–12656.
30. Hayashi I, et al. (2007) Crystallographic evidence for water-assisted photo-induced peptide cleavage in the stony coral fluorescent protein Kaede. *J Mol Biol* 372:918–926.
31. van Thor JJ, Gensch T, Hellingwerf KJ, Johnson LN (2002) Phototransformation of green fluorescent protein with UV and visible light leads to decarboxylation of glutamate 222. *Nat Struct Biol* 9:37–41.
32. Chudakov DM, et al. (2003) Kindling fluorescent proteins for precise in vivo photolabeling. *Nat Biotechnol* 21:191–194.
33. Stiel AC, et al. (2007) 1.8 Å bright-state structure of the reversibly switchable fluorescent protein Dronpa guides the generation of fast switching variants. *Biochem J* 402:35–42.
34. Cotlet M, et al. (2001) Identification of different emitting species in the red fluorescent protein DsRed by means of ensemble and single-molecule spectroscopy. *Proc Natl Acad Sci USA* 98:14398–14403.
35. Marchant JS, Stutzmann GE, Leissing MA, LaFerla FM, Parker I (2001) Multiphoton-evoked color change of DsRed as an optical highlighter for cellular and subcellular labeling. *Nat Biotechnol* 19:645–649.
36. Matsuda T, Miyawaki A, Nagai T (2008) Direct measurement of protein dynamics inside cells using a rationally designed photoconvertible protein. *Nat Methods* 5:339–345.
37. Bourgeois D, Vernède X, Adam V, Fioravanti E, Ursby T (2002) A microspectrophotometer for UV-visible and fluorescence studies of protein crystals. *J Appl Crystallogr* 35:319–326.
38. Field MJ, Albe M, Bret C, Proust-de-Martin F, Thomas A (2000) The dynamo library for molecular simulations using hybrid quantum mechanical and molecular mechanical potentials. *J Comput Chem* 21:1088–1100.